Thermogravimetric study on thermal degradation kinetics and polymer interactions in mixed thermoplastics

N. Netsch[1] · L. Schröder[1] · M. Zeller[1] · I. Neugber[1] · D. Merz[1] · C. O. Klein[2] · S. Tavakkol[1] · D. Stapf[1]

Abstract

Potential interactions during thermal degradation of polymer blends significantly influence product yields and their composition. Therefore, chemical recycling of plastic waste requires fundamental understanding of feedstock dependency for effective process design. This study investigates the pyrolysis of polymer blends (HDPE, LDPE, PP, PS, ABS, PET, PA6, PVC) through thermogravimetric experiments at different heating rates. Sample homogeneity's impact on interactions is analyzed using particles, powder, coextruded blends, and samples in crucibles with separated compartments. A kinetic model is presented to support the experimental findings, assuming linear superposition of individual polymer kinetics. A proposed grouping of thermoplastics, reflecting their degradation behavior and potential interactions, correlates with the polymer structure. Observed interactions, particularly in blends of heteroatom-containing polymers (N, O, Cl), are accelerated reactions and coke formation. Hence, the model accurately predicts the degradation of heteroatom-free polymer mixtures but encounters challenges with more complex blends. This comprehensive study emphasizes the importance of feedstock composition for future pyrolytic polymer recycling.

Graphical abstract
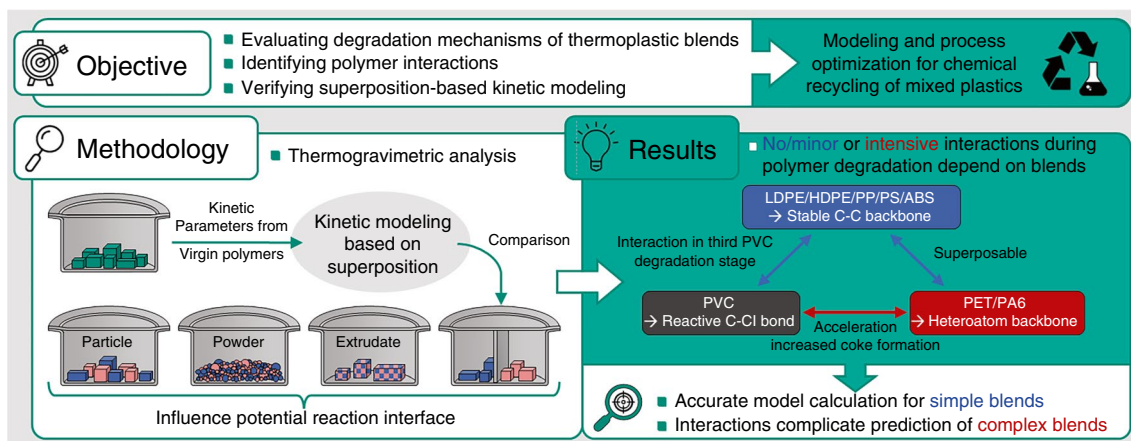
Keywords Thermoplastics · Pyrolysis · Thermogravimetry · Thermal degradation · Kinetic modeling · Decomposition interaction

Abbreviations

ABS	Acrylonitrile butadiene styrene	PE	Polyethylene
HDPE	High-density polyethylene	PET	Polyethylene terephthalate
LDPE	Low-density polyethylene	PP	Polypropylene
PA	Polyamide	PS	Polystyrene
		PVC	Polyvinyl chloride

Extended author information available on the last page of the article

RMSD   Root mean square deviation
TG   Thermogravimetry

Introduction

The transformation from linear value chains to a circular economy offers the advantage of growing independence from fossil raw materials and reduced CO_2 emissions [1]. The European Union has proclaimed carbon net zero as the main objective of future economic actions [2]. To reach this target, the production of polymers and the management of plastic waste have to become substantially resource-efficient [3, 4]. The recycling of plastic waste is preferable to its energetic use or landfilling to reduce the ecological footprint [5–8]. Mechanical plastics recycling is well established, leading to a global recycling rate of 24 mass% in 2014 [9]. Nevertheless, many plastic-rich waste fractions cannot be mechanically recycled, which is why chemical recycling is a useful complementary process [10]. Pyrolysis, the thermal degradation in inert atmosphere, gains focus as thermochemical recycling option [11].

Plastic wastes are heterogeneous mixtures of different types of plastic. Also, they may contain other adhesions such as biomass or inorganic components [12, 13]. Nevertheless, since a few thermoplastics dominate the plastic production these polymers are largely represented in the waste feedstocks relevant for the recycling via pyrolysis. These polymers are polyethylene (PE), polypropylene (PP), polystyrene (PS), polyvinyl chloride (PVC), polyethylene terephthalate (PET), acrylonitrile butadiene styrene (ABS), and polyamide (PA) [14]. The pyrolysis of PE, PP, PS, and ABS follows complex single-step radical reaction mechanisms [15–18]. In these mechanisms, radicals are initially generated by homolytic bond cleavage, which proceeds to a preparation phase in which the radicals react with polymer chains and cause further cleavages. The mechanism terminates with the recombination of the radicals. Depending on the polymer type, the mechanisms favor bond cleavage at varying chain positions, which leads to significant different product compositions. PET and PA undergo single-step degradation initiated by ionic intramolecular transfer reactions [19–22]. Thermal degradation of all these polymers occurs at temperatures above 670 K, typically. Significant amounts of solid pyrolysis residue, considered as coke, are generated when pyrolyzing PET. The coke is formed during the degradation reaction while emitting oxygen-containing volatiles from the polymeric structure, e.g., CO_2 or carboxylic acids, resulting in polycyclic and polyaromatic structures. PVC degrades in a three-step radical chain scission with HCl formation in the first degradation step starting at approximately 520 K, already [23, 24]. The three-step mechanism results from the significant bond stability variations of the carbon–carbon and chlorine–carbon bonds that build the polymeric PVC structure. This first step is followed by hydrocarbon volatilization and polyene intermediate formation. These unsaturated polyene chains ultimately degrade producing coke and volatile hydrocarbons with mostly aromatic structures. The coke is formed by cross-linking of the polyene chains.

Knowledge of the detailed degradation behavior enables process design and optimization. For pyrolysis, kinetic modeling is often based on experimental data and simplified model assumptions due to the complexity of degradation mechanisms. The pyrolysis kinetics are valid for the range of substances under investigation. For example, the multistage degradation of various polyurethanes can be represented with the n-th order model approach of Zeller et al. [25]. Also, Aboulkas et al. successfully applied this approach to HDPE, LDPE, and PP [26]. An application-oriented modeling technique to describe the degradation kinetics of mixtures based on the superposition of pure substance properties appears promising. Different authors negate significant mixing effects on the degradation products for various polymer blends. Mixtures of PE, PP, and PS can be described well via superposition according to Westerhout et al. [27]. This result is confirmed by Costa et al. and Faravelli et al. for PE-PP and PE-PS mixtures, respectively [28, 29]. Wu et al. proved that the degradation behavior of PVC-PE blends can be well represented with this linear superposition approach [30]. Even when Genuino et al. identified limitations by linear superposition of data, the approach was successfully applied for plastic mixtures of HDPE, LDPE, PP, PS, and PET to predict the product yields [31]. Interactions during co-pyrolysis are therefore often considered neglectable for specific blends.

Basically, when pyrolyzing plastic mixtures the resulting intermediates from one polymer can react with degradation intermediates of another one [32]. These interactions between polymer products may ultimately influence the product distribution, but also the degradation kinetics. In such cases, linear postponed approaches for degradation kinetics of mixtures are invalid [33]. When co-pyrolyzing polyolefins, slight acceleration in the thermal degradation compared to pure substances is reported [34, 35]. Genuino et al. found the formation of solid products increased beyond expectations when adding low amounts of PET to polyolefins and PS in a batch reactor [31]. This effect is confirmed by Hujuri et al. who additionally observed a synergistic effect as LDPE and PP degrade at lower temperatures when mixed with PET [36]. Therefore, they suggest an interaction term in superposition-based kinetic modeling. Contrary behavior is reported when pyrolyzing PVC in blends with PE, PP, and PS. Yu et al. summarized the degradation of polyolefins and PS being delayed because of PVC intermediates. Increased coke formation is observed [23], which is confirmed in vacuum pyrolysis in a batch reactor [37].

Miranda et al. also identified PVC and PS as responsible for interactions in the pyrolysis of their feedstocks. Therefore, Tuffi et al. proposed three criteria directly influencing potential interactions [38]. First, interaction is more present if polymers are pyrolyzed which feature similar onset temperatures of degradation. Second, the dependency of the polymer concentration is underlined. At last, the homogeneity of the blend emerges as a crucial factor for degradation kinetics. Faravelli et al. emphasized this factor of interfacial effects in the material system [29].

Concluding, a majority of the literature assumes interactions during the co-pyrolysis of mixed thermoplastics but conflicting degradation phenomena during thermoplastic co-pyrolysis are reported. Also, PA and ABS are rarely investigated in detailed mixed plastic studies. Most of the models published for the degradation kinetics are tailored for specific polymers or limited to only two or three polymers in the mixture. This systematic thermogravimetric investigation covers a broad polymer portfolio, namely LDPE, HDPE, PP, PS, ABS, PET, PA6, and PVC. Thus, this work aims to clarify the pyrolysis behavior of blends which include the major thermoplastics in plastic waste. Polymer interactions during degradation are investigated depending on the polymer type, its concentration, and the homogeneity of the sample mixture. The role of the interface available for interactions during the reactions is in focus. Differently prepared polymer samples allow a comparison of the interface influence based on spatial proximity. A superposition-based kinetic model is adapted by extending the kinetic modeling methodology of Zeller et al. from virgin plastics to thermoplastic blends [25]. In addition to the theoretical calculations based on a superposition approach, novel crucibles with divided compartments are used as defined control experiments. The applicability of this approach is validated by systematic comparison to the comprehensive experimental dataset.

Materials and experimental methods

In this study, eight thermoplastics were tested, namely Hostalen ACP 9255 Plus (HDPE), Lupolen 24020H (LDPE), Moplen HP 552H (PP), each from LyondellBasell industries, Styrolution 156F (PS) from INEOS Styrolution, Sinkral F332 (ABS) by Eni, and Alphalon 27 (PA6) by Grupa Azoty. PET is supplied by Plastikpak Italia Preforme. The thermoplastics were acquired as granules, except for Primex P2252 (PVC) which was delivered as powder by Mexichem. All polymers are free of additives, e.g., flame retardants, inorganic fillers, or UV stabilizers. The elemental analyses, ash and moisture content, higher heating values (HHV), and lower heating values (LHV) are listed in Table 1.

Thermogravimetry (TG) was carried out on a NETZSCH TG 209 F1 Libra equipped with an autosampler. The pyrolysis was performed from 303 to 1173 K and at constant heating rates of 2, 5, 10, 20, and 40 K min^{-1} in nitrogen atmosphere. The nitrogen flow rate was set to 60 mL min^{-1}. Reproducibility could be confirmed in five tests per plastic type at 10 K min^{-1}. All other experiments were conducted twice and averaged. The samples were introduced in Al$_2$O$_3$ crucibles. The total sample mass accounts for 10 mg deviating only up to 0,1 mg. Following the ICTAC recommendations, the heating rate and sample mass were selected to prevent temperature errors [39]. Binary plastic blends were prepared with shares of 75/25 mass%, 50/50 mass%, and 75/25 mass%. Binary blends reach 28 plastic-type configurations by combining each of the eight polymers. The preparation of each component's sample mass only deviated 10–15 µg of the set value in the mixture. In the experiments, the heating rate was kept constant at 10 K min^{-1}.

The samples were added as small particles sliced from the primary granules using a scalpel. Therefore, the particle size was not uniform and varied in shape and mass between 0.5 and 5 mg of each particle slice. The influence on degradation

Table 1 Elemental analyses of the investigated polymers including heating values, moisture, and ash content

Polymer	Elemental analysis/mass%							Heating value/MJ kg^{-1}		
	C	H	N	Cl	Moisture	Ash	O[a]	LHV[b]	HHV[b]	HHV[c]
LDPE	85.8	14.2	0.0	0.0	0.0	0.0	0.0	43.2	46.3	46.3
HDPE	85.8	14.2	0.0	0.0	0.0	0.0	0.0	43.2	46.3	46.1
PP	85.8	14.2	0.0	0.0	0.0	0.0	0.0	43.2	46.3	46.1
PS	92.0	8.0	0.0	0.0	0.0	0.0	0.0	39.5	41.3	41.3
ABS	86.2	8.0	5.5	0.0	0.3	0.0	0.0	37.9	39.6	39.6
PET	63.3	4.4	0.0	0.0	0.2	0.0	32.1	22.7	23.7	22.9
PA6	63.6	9.8	12.6	0.0	1.3	0.0	12.7	30.8	33.0	31.2
PVC	39.6	5.6	0.0	54.7	0.1	0.0	0.0	19.0	20.3	-

[a] Calculated as difference to 100 mass%

[b] Calculated from elemental analysis

[c] Determined experimentally

interactions by the polymer arrangement within the mixture was tested. For this purpose, three different sample arrangements were compared: particles, powder, and coextruded samples. In any case, the sample preparation was performed by minimizing the energy input into the material to prevent the samples from aging, e.g., by thermal stress. The powders were obtained by crushing the granules to < 500 μm in a rotor mill. Thermally induced degradation of the polymers was avoided by cooling the granulate and the rotor mill with liquid nitrogen [40, 41]. Powder samples were used in TG after manual mixing in the crucibles in the specific ratio. Powder experiments investigated homogeneous blends on a macroscopic level. Extrudate was generated by co-extruding the powder of pure plastics or premixed powder blends in a micro-extruder (Haake MiniLab 3 micro-compounder) by ThermoFisher Scientific. Coextruded samples represent a microscopic homogeneous mixture with maximum contact of the different polymer chains. Because of the varying melting and degradation temperatures and limited miscibility of the polymers, extruded samples were generated for pure LDPE, HDPE, PP, PS, ABS, PET, PA6, and 50/50 blends of LDPE/PP, LDPE/PS, PS/ABS, and PET/PA6. PVC powder could not be extruded because even at low temperatures visual changes of the polymer occurred. The dwell time in the extruder was set to 3 min. The extrusion temperature was selected as low as possible to prevent changes in the samples. The temperature it therefore adapted to the polymer properties. LDPE/PP was processed at 433 K and PET/PA6 at 523 K. Both other mixtures were extruded at 473 K. In contrast to extruded samples, control experiments with polymers were conducted avoiding any possible reaction interface. Crucibles of identical dimensions were used. These crucibles feature one additional wall that separates the sample into different compartments for each polymer of the mixture.

In addition to the binary mixtures, a particular blend of LDPE, HDPE, PP, PS, and ABS with 20 mass% each was tested (Mix 1). A blend of all thermoplastics (Mix 2) with 20 mass% LDPE and HDPE, and 10 mass% each of PP, PS, ABS, PET, PA 6, and PVC was also pyrolyzed under identical conditions.

Theory and calculations

Kinetic models describing the degradation of polymers can either use model-free approaches or model-based approaches. The model for predicting the reaction kinetics of thermoplastic mixtures is based on the independent parallel reactions model introduced by Jomaa et al. [42]. The model was refined by Zeller et al. [25]. Each independent reaction represents a pseudo-reaction j of polymer i, which describes a degradation stage of this polymer apparent in

the TG data. The reaction conversion α of the polymer is formulated following an Arrhenius approach. The time-dependent conversion rate of a pseudo-reaction is therefore described, as shown in Eq. 1. It includes the kinetic triplet of activation energy $E_{A i,j}$, preexponential factor $k_{0,i,j}$, and kinetic model $f(\alpha_{i,j})$.

$$\frac{d\alpha_{i,j}}{dt} = k_{0,i,j} \cdot f\left(\alpha_{i,j}\right) \exp\left(-\frac{E_{A,i,j}}{RT}\right) \tag{1}$$

Several options are proposed for the kinetic model term [39, 43, 44]. In this work, a n-th order model is assumed. Therefore, a term for the reaction order $n_{i,j}$ is added as an additional parameter to the kinetic triplet, as shown in Eq. 2.

$$f\left(\alpha_{i,j}\right) = \left(1 - \alpha_{i,j}\right)^{n_{i,j}} \tag{2}$$

Most of the thermoplastics investigated in this study include one pseudo-reaction due to the one-step degradation mechanism. PA6 and PVC are an exception. A low mass loss that precedes the degradation of PA6 results in the addition of a second pseudo-reaction. For PVC, three reactions are implemented because of the two-stage degradation with a split first degradation step [23]. Accordingly, the number of pseudo-reactions is adapted to polymer-specific experimental results. The number of pseudo-reactions is additionally validated by the conversion-dependent illustration of activation energy and the preexponential factor according to the model-free method of Kissinger–Akahira–Sunose (KAS). This method follows the recommendations of the ICTAC committee [39]. These plots can be found in the supplementary information. The share of multiple pseudo-reactions is considered by introducing the reaction fraction $q_{j,i}$ as following.

$$\frac{d\alpha_i}{dt} = \sum_j q_{i,j} \cdot k_{0,i,j} \cdot f\left(\alpha_{i,j}\right) \exp\left(-\frac{E_{A,i,j}}{RT}\right) \tag{3}$$

The time-dependent conversion $\alpha_i(t)$ is defined as a function of the mass at a specific time $m(t)$ of the experiment. The sample mass at the beginning m_0 and at the end m_∞ is also implemented according to formula 4. The kinetic parameters are calculated analogously to Zeller et al. using the pattern search algorithm in MATLAB [25].

$$\alpha_i(t) = \frac{m_0 - m(t)}{m_0 - m_\infty} \tag{4}$$

The volatile formation $m_V(t)$ represents the complement of the solid mass loss $m_S(t)$. In contrast to the conversion, these characteristic values also indicate the solid residue generated in the TG experiments. They are calculated as described in formula 5.

$$m_{\mathrm{V}}(t) = 1 - m_{\mathrm{S}}(t) = 1 - \frac{m(t)}{m_0} \tag{5}$$

The optimized determination of the kinetic parameters of the respective polymers follows the recommendations of the ICTAC kinetics committee [39]. It is based on the averaged datasets at different heating rates. The conversion rate of the degrading polymer mixtures α_{Mix} is calculated concerning the polymer mass fraction in the mixture x_i. Linear superposition of the individual polymer kinetics is used according to formula 6. The model is valid for non-isothermal experiments with a constant heating rate of 2 to 40 K min^{-1}.

$$\frac{\mathrm{d}\alpha_{\mathrm{Mix}}}{\mathrm{d}t} =$$
$$\sum_i \left(x_i a_i(t) \right) = \sum_i x_i \sum_j q_{i,j} \cdot k_{0,i,j} \cdot \left(1 - \alpha_{i,j} \right)^{n_{i,j}} \exp \tag{6}$$
$$\left(-\frac{E_{\mathrm{A},i,j}}{RT} \right)$$

The pattern search algorithm in MATLAB [45] was applied to etermine optimal kinetic parameters to fit the experimental data. The root mean square deviation (RMSD) is introduced as a metric to evaluate the model's accuracy by comparing the deviation of experimental and model results. The calculation of the RMSD of z datapoints from experimental mass loss $b_{\mathrm{exp},k}$ and modeled mass loss $b_{\mathrm{model},k}$ is described according to formula 7. In this study, the RMSD is determined for the mass loss in the temperature range of 313–1123 K with increments of 0.25 K.

$$\mathrm{RMSD} = \sqrt{\frac{1}{z} \sum_k \left(b_{\mathrm{exp},k} - b_{\mathrm{model},k} \right)^2} \tag{7}$$

Results and discussion

Pure polymers

Concerning the chemical recycling of plastics, the volatile pyrolysis products of condensed and permanent gases are of importance. Thus, instead of the mass loss curve, the temperature-related formation of volatiles is shown in Fig. 1. Volatile formation curves at a heating rate of 10 K min^{-1} of the pure thermoplastics are displayed. However, these curves can be easily converted into mass loss curves using Eq. 5. The polymers heating rate-dependent onset temperature, respectively, for each degradation stage, can be sorted from low to high values as following:

PA6 I < PVC I < PVC II << PS < ABS < PET

< PA6 II < PP < PVC III < LDPE < HDPE

All polymers show a single-step degradation mechanism, except for PVC which features a three-step mechanism. Pyrolysis of PET and PVC leads to considerable coke formation of 12.0 mass% and 6.6 mass%, respectively. For ABS and PA6, minor solid amounts of 0.3 and 0.2 mass% are obtained. Coke formation of the other thermoplastics is neglectable since it accounts for less than 0,1 mass% in these investigations. In the variation of the heating rate from 2 to 40 K min^{-1}, no influence of the heating rate on the generated share of coke is identified.

The degradation shifts toward higher temperatures with increase in heating rates. This effect is often attributed to the phenomena of thermal lag. Thermal lag describes the delay of temperature measurement in the sample and the sensor due to thermal transport phenomena [46]. The effect is dependent on the device and the thermal properties of the sample, more precisely the thermal conductivity and heat capacity. Since the properties of the polymers are similar, the effect of thermal lag is comparable and mostly depends on the heating rate applied in the experiments. Because low heating rates are used, the time–temperature correlation is a more reasonable cause for the shift. At lower heating rates, the sample stays longer at a specific temperature. With the respective kinetic, the conversion is higher in the longer time interval. This results in the supposed shift of the curve to lower temperatures.

From the experimental dataset, kinetic parameters are derived according to the methodology of Zeller et al. [25]. The dataset including five heating rates was used for kinetic parameter determination with the pattern search algorithm. Table 2 lists the preexponential factor, activation energy, and reaction order. The reaction fraction of individual reactions in a multi-step degradation is also shown. The results match relevant literature [15, 22, 26, 47–51]. Except for the initial outgassing of PA6 and the third PVC stage, the reaction order varies between 0.9 and 1.1 for all polymers and degradation steps.

With the derived kinetic parameters, the degradation of pure plastics is modeled. In Fig. 1, experimental and modeled data are compared at a heating rate of 10 K min^{-1}. The data for the comparison at heating rates of 2, 5, 20, and 40 K min^{-1} and the corresponding RMSD values can be found in the supplementary information. Additionally, the capability of model extrapolation was tested by comparing its results to data acquired in experiments with a heating rate of 100 K min^{-1}. Since the kinetic parameters are valid for a heating rate range from 2 to 40 K min^{-1} differences are to be expected. The data and a summarizing figure are included in the supplementary information. For LDPE, PS, and ABS, the model shows a similar RSMD to the results in obtained at 2–40 K min^{-1}. For PET and PA6, the model
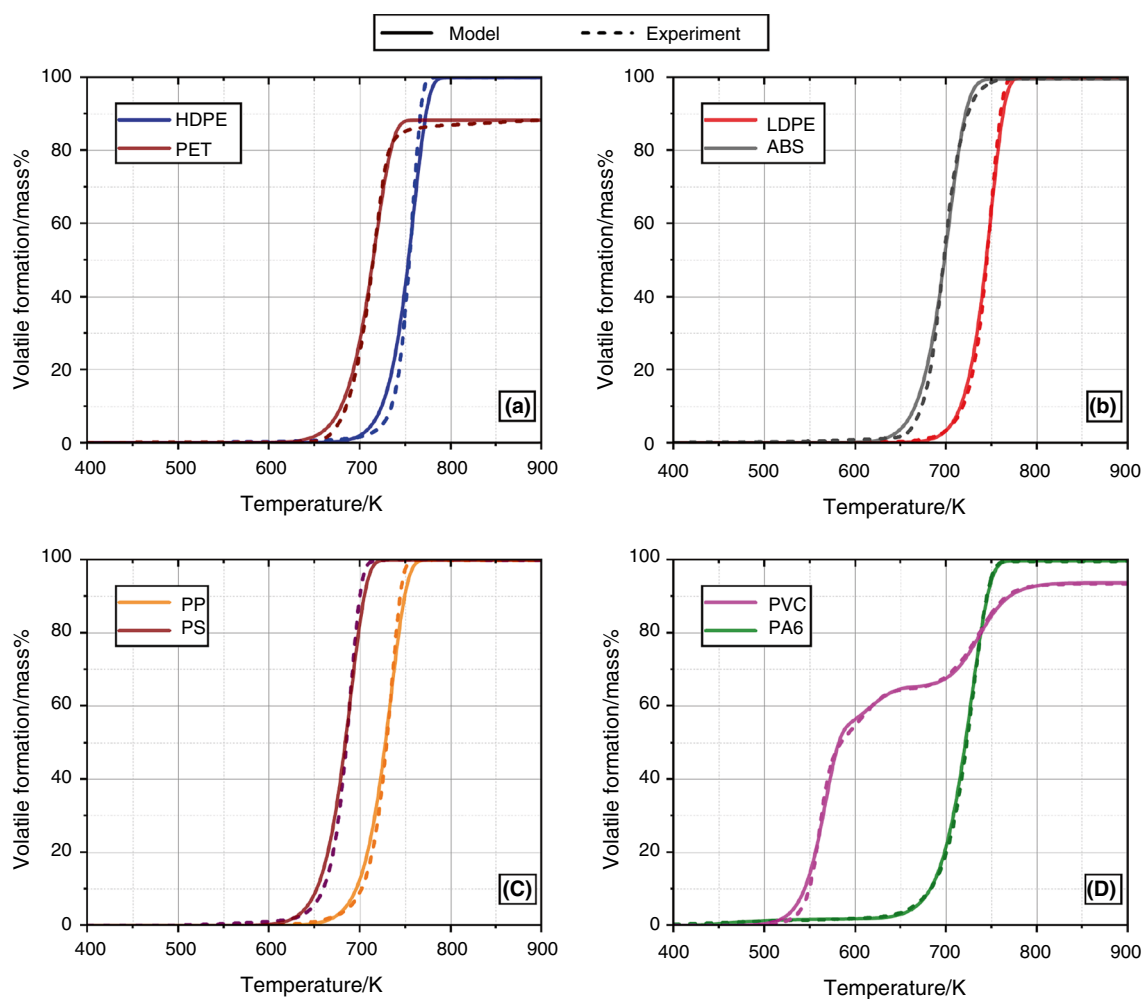
Fig. 1 Experimental and modeled volatile formation from particular sample of HDPE and PET **A**, LDPE and ABS **B**, PP and PS **C**, and PVC and PA6 **D** at a heating rate of 10 K min^{-1}

Table 2 Kinetic parameters derived from TG experiments of pure polymers at constant heating rates between 2 and 40 K min^{-1}

Polymer	Preexponential factor k_0/s^{-1}	Activation energy E_A/ kJ•mol^{-1}	Reaction order n/-	Reaction fraction q/-
LDPE	$3.80 \cdot 10^{17}$	281	0.94	1.00
HDPE	$8.31 \cdot 10^{16}$	275	0.94	1.00
PP	$3.32 \cdot 10^{14}$	233	0.94	1.00
PS	$6.37 \cdot 10^{13}$	209	0.94	1.00
ABS	$1.22 \cdot 10^{14}$	217	1.08	1.00
PET	$1.46 \cdot 10^{13}$	209	0.93	0.99
PA6 I	$2.11 \cdot 10^{8}$	92	3.00	0.02
PA6 II	$3.02 \cdot 10^{12}$	203	0.93	0.98
PVC I	$1.35 \cdot 10^{13}$	164	0.94	0.53
PVC II	$2.98 \cdot 10^{6}$	103	0.92	0.16
PVC III	$1.89 \cdot 10^{16}$	257	1.97	0.31

replicates the experimental results with minor deviations while PVC modeling exhibits more significant differences. These differences refer to the second degradation stage which compared to the first and third degradation stages of PVC is not replicated precisely. The model extrapolation to higher heating rates is therefore limited and depends on the polymer. In the heating rate validity range, the degradation of single-step pyrolyzing polymers is replicated well for the range of 10 to 90% of the conversion. The model accuracy is polymer dependent resulting in RMSD between 0.4 mass% (for PA6) and 2.2 mass% (HDPE). Most inaccuracies are present at the start and the end of the conversion, especially for HDPE, PET, ABS, and PS. The calculated initial mass loss of PA6 corresponds to the experimental data. For PVC, the first and the second degradation stages occur at temperatures between 520 and 620 K. Both, the first and the second stages overlap merging their transition. This effect is more pronounced in experiments than in the model and at lower heating rates. The RMSD for PVC is therefore

higher when comparing the model with experimental results with heating rates of 2 K min^{-1} (RMSD 1.7 mass%) and 40 K min^{-1} (RMSD 1.5 mass%) to the medium heating rate of 10 K min^{-1} (RMSD = 0.8). The third degradation step occurs at significantly higher temperatures over 700 K. This leads to a characteristic plateau at about 70 mass% mass loss independent of the heating rate. All stages are described well by the model. Consequently, this comparably straightforward model enables reliable simulation of pyrolytic mass loss in TG for all pure polymers in the validity range of heating rates over a broad range of the conversion process (approximately 10–90%). This may be explained by the underlying reaction mechanism. The radical degradation mechanisms require initiation reactions in the form of homolytic bond cleavage to generate the first radicals. The end of the mechanism is characterized by the recombination of radicals. In these phases, the reaction accelerates and slows down. In the conversion range of 10 to 90%, the reaction then reaches a stable level, as new radicals are generated, the main propagation phase takes place and free radicals recombine at the same time.

The influence of sample processing was investigated. Figure 2 exemplarily shows the comparison of different preprocessed LDPE and PET samples. Multiple tests with differently processed samples again emphasize the reproducibility of the experimental setup and no influence of the sample preparation with pure polymer experiments. The volatile formation curve and the final solid residue remain unchanged after shredding or extruding. The RMSD for differently prepared pure polymers is similar considering the margin of error. Short dwell time, cryo-cooling while shredding, and minimal extrusion temperatures prevent thermal degradation of the polymers or moisture-induced hydrolysis of PET during sample preparation [52]. Therefore, no influence of the sample preparation was present for LDPE and

PET. The same result was observed during testing HDPE, PP, PS, ABS, and PA6. Extrusion of PVC leads to significant changes in the polymer appearance which is why the experiments with extruded PVC are not conducted.

Binary polymer mixtures

The systematic study of binary mixtures reveals potential interaction effects during thermal degradation between the investigated polymers. To evaluate potential interaction, multiple criteria are considered. Interaction is proposed if the degradation of blends characterized by the volatile formation curve differs from model data and control experiments. For this purpose, the onset of the degradation mechanism, the completed conversion at characteristic temperatures, peak intensity, peaks in the differential volatile formation curves, or the solid residue mass is consulted.

The test matrix of 28 different polymer mixtures, each with three different mixing ratios, allows the polymers to be grouped. Three different groups for the investigated feedstocks are proposed. The groups are listed in Table 3. Polymers of the same group show similar behavior regarding interaction effects. In addition, exemplary mixtures with different sample homogeneity indicate influences of the polymer chain spatial proximity on the degradation.

Group I includes polymers with a chain backbone only composed of carbon–carbon bonds. This group consists of LDPE, HDPE, PP, PS, and ABS. Figure 3 shows exemplary curves of various binary blends within this group. As with the pure polymers, neglectable solid residue is formed in the mixtures of Group I. Similar to LDPE/PP blends, LDPE/HDPE, HDPE/PP, and PS/ABS also show a single-step degradation. The degradation occurs within the temperature range of the pure substance's degradation. It shifts with increase in concentration of the polymer toward its
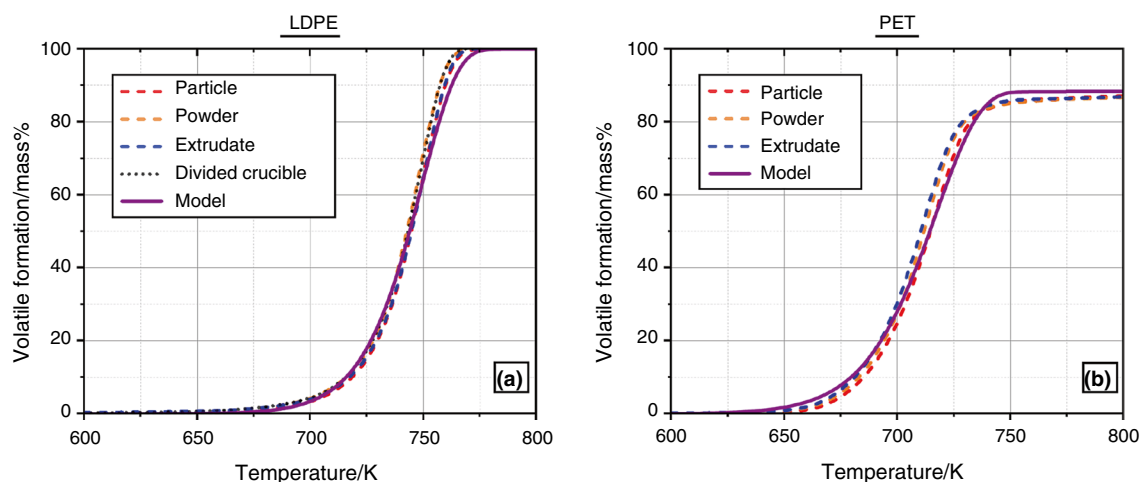
Fig. 2 Temperature-dependent volatile formation compared for differently prepared LDPE **A** and PET **B** samples at a heating rate of 10 K min^{-1}

Table 3 Proposed grouping of the investigated thermoplastics considering their degradation behavior and characteristic structure

	Polymers	Characteristic structure
Group I	LDPE, HDPE, PP, PS, ABS	Chain backbone of carbon–carbon bonds
Group II	PET, PA6	Chain backbone of carbon together with oxygen or nitrogen atoms
Group III	PVC	Carbon-containing chain backbone with multiple chlorine atoms as pendant groups

degradation curve. A mechanism with two strongly overlapping peaks can be assumed from the differential volatile formation curves in Fig. 3B. Those peaks serve as indicators of degradation stages. Multiple peaks emphasize the occurrence of multiple degradation stages which are also indicated by inflection points in the volatile formation curve. The RMSD of binary mixtures from polymers in Group I shows no or only minor deviations between the model and experimental results. Therefore, the model reproduces the curves in Fig. 3 well within the model deviations already evaluated with pure polymers.

The mixtures of HDPE/PS, HDPE/ABS, and LDPE/PS show a two-stage degradation with an inflection point. The temperature of the inflection point correlates closely with the mixing ratio. The volatile formation rate of these blends exhibits two different peaks correlating to each polymer as shown for LDPE/PS blends in Fig. 3. The first peak corresponds to the PS degradation, while the peak between 700 and 775 K can be attributed to LDPE. The onset of each polymer's degradation explains the partly varying shaped curves of the blends. If the onset temperature of the pure polymers is similar, as is the case with LDPE/PP, no stages emerge as a result of the proximity of differential TG peaks. Thus, inflection points in the volatile formation rate and an apparent two-stage mechanism only appear in plastic blends of polymers with a significant difference in the degradation onset temperature.

This result is confirmed by the data for LDPE/ABS, PP/PS, and PP/ABS. These blends show moderate differences in the onset temperature within polymer Group I. As depicted for PP/PS blends in Fig. 3, inflection points are only slightly pronounced and peaks in the volatile formation rate are overlapping. Nevertheless, two peaks corresponding to PS (650–725 K) and PP (700–760 K) are visible. In general, the inflection points indicate an independence of the individual polymer degradation within the mixture. In comparison with the superposition model, however, an acceleration of the polymer's degradation with a higher onset is evident, leading to slightly increased RMSD for LDPE/PP, LDPE/PS HDPE/PP, HDPE/PS, and PP/PS mixtures. Like with LDPE/PS, this acceleration is also more pronounced when the onset temperature varies significantly. This behavior can be attributed to the molecular structure and, thus, the degradation mechanisms. All polymers of Group I pyrolyze

via radical chain scission. This mechanism requires an initial reaction of homolytic bond cleavage. Aromatic or alkyl side groups stabilize these starting radicals, resulting in their formation at lower temperatures in PS, ABS, or PP than in HDPE or LDPE [16, 27]. Radicals from the earlier degrading component are present in the mixtures and may function as initial radicals for the degradation mechanism of the other component. The influence of the potential interaction interface on the degradation of LDPE/PS blends in a ratio of 50/50 is shown in Fig. 4. TG curves are shifted toward lower temperatures compared to samples of control experiments with the separated crucible compartments. This effect is indicated by the RMSD which is significantly lower for control experiments than for samples with a shared reaction room. The shift is comparable for all mixtures independently from sample preparation. With the mixing ratio of 50/50 mass%, this acceleration occurs at approximately 50% conversion rate. As a consequence, the model calculations are below the experimental results at the end of the degradation curve. However, the dependence of the TG curve on the onset temperature remains more pronounced than the sample preparation for Group I blends. Therefore, no clear dependency between the reaction acceleration and the proportions of the polymers in the mixture is evident. In conclusion, only minor interactions regarding the degradation kinetics were observed. These are characterized by a slight acceleration of the degradation reaction of the polymer with a higher onset temperature. Thus, the degradation is well described using the superposition model.

Group II is defined as consisting of polymers with additional heteroatoms in the chain backbone, like PET (oxygen) or PA6 (nitrogen). The volatile formation of these blends is shown in Fig. 5A. The blends exhibit differing degradation behavior compared to control experiments or linear postponed model results. The volatile formation in the temperature range from 695 to 775 K accounts for approx. 70 mass% in the model and the experiments with divided crucibles, while only 20% are formed below 629 K. In the particle, powder, and extruded samples, the volatile formation shifts to lower temperature exhibiting approx. 80 mass% of volatiles formed before reaching 695 K. This reaction acceleration of up to 60 K leads to a significant increase of the RMSD to 7.3 mass% to 11.6 mass%. Figure 5B shows a strong influence on the sample mixture intensity. The
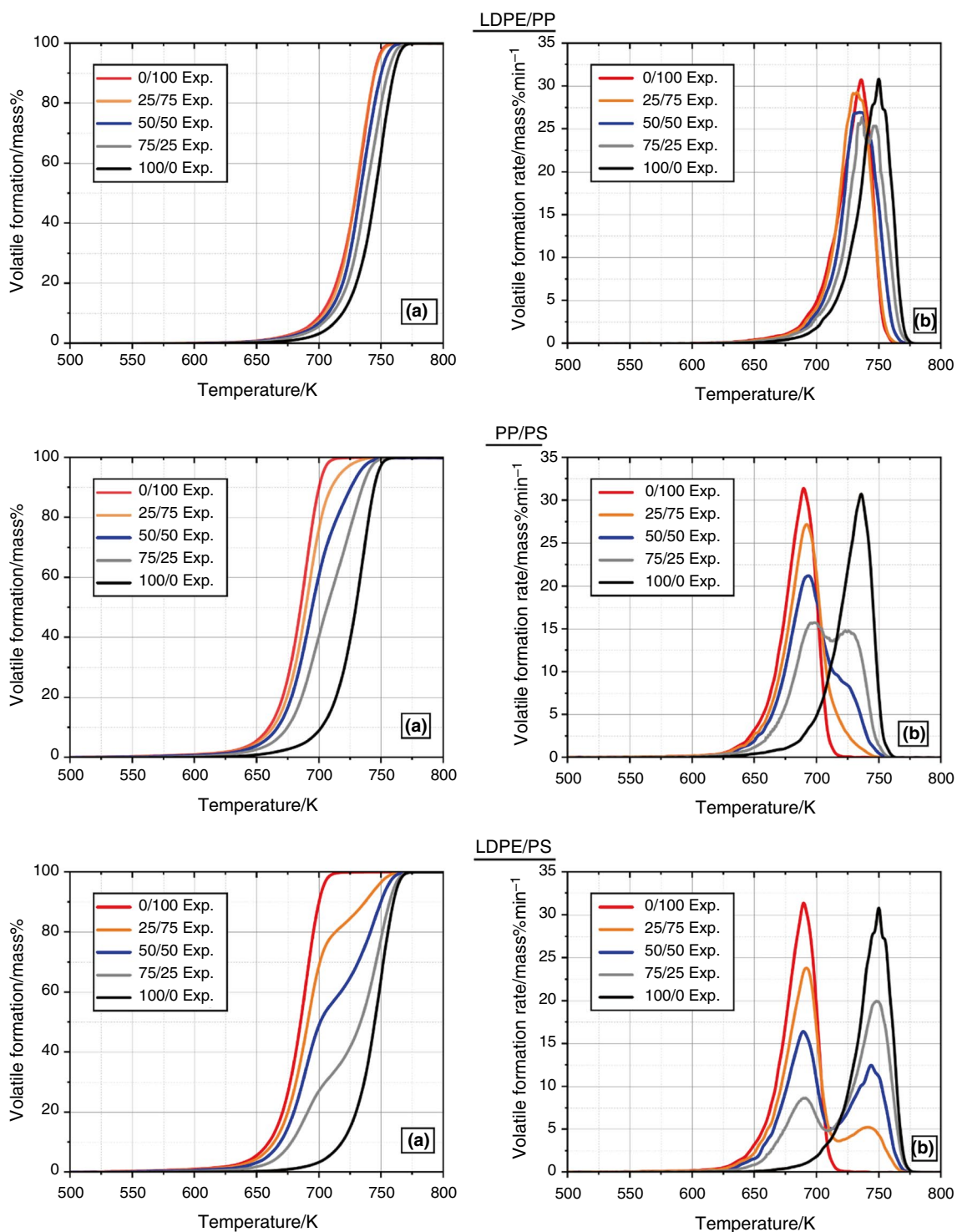
Fig. 3 Volatile formation **A** and its formation rate **B** of particular LDPE/PP, PP/PS, and LDPE/PS blends at mixing ratios 0/100, 25/75, 50/50, 75/25, and 100/0 mass% at a heating rate of 10 K min^{-1}

accelerated conversion is more pronounced for extrudates than for powders. In turn, the latter shows a stronger shift than the particles. Interactions of the polymers in the degradation intensify with increase in sample homogeneity and thus the potential reaction interface of the polymers. Results of extruded, powdered, and particular blends of PA6 and PET differ significantly from the sample in separated crucible compartments of control experiments. This indicated
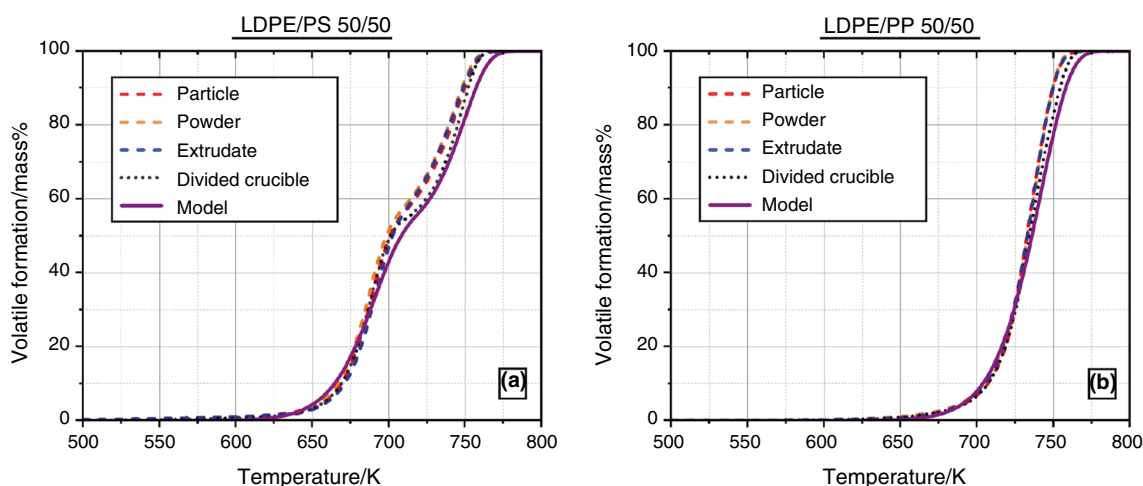
Fig. 4 Volatile formation in differently prepared LDPE/PS **A** and LDPE/PP **B** blend samples in the ratio of 50/50 mass% covering multiple homogeneity grades at a heating rate of 10 K min^{-1}
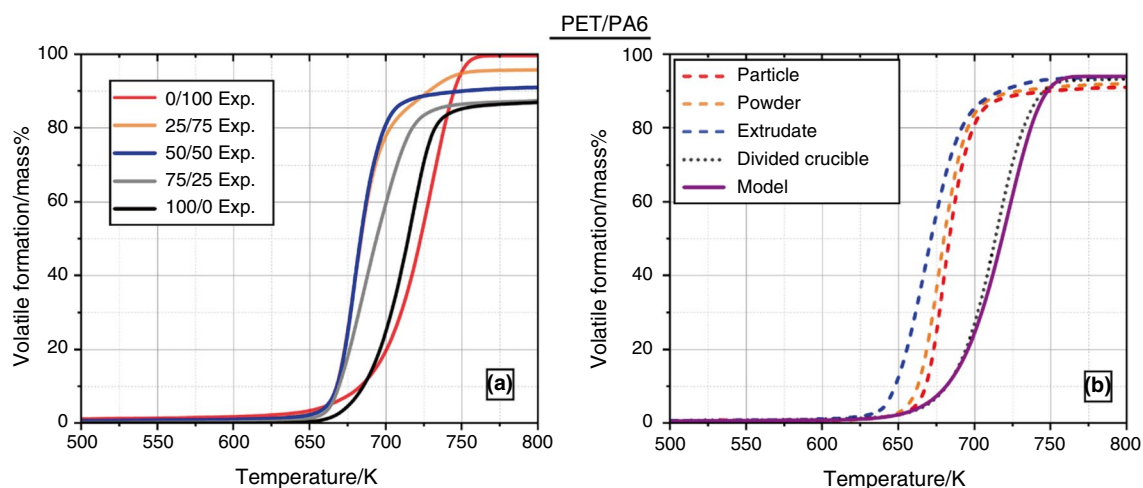
Fig. 5 Volatile formation from particular PET/PA6 mixtures in the ratio of 0/100, 25/75, 50/50, 75/25, and 100/0 mass% **A** and the comparison of the mixing intensity on 50/50 blends **B** at a heating rate of 10 K min^{-1}

significant interactions and changes in the degradation mechanism. The reaction mechanism of these polymers that involves intramolecular ionic transfer reactions resulting in carboxylic acids from PET degradation can therefore interfere with the mechanism of PA6 degradation [53]. Conversely, the presence of ε-caprolactam and the outgassing components of PA6 may accelerate PET degradation. As a result of the strong interactions, the superposition-based modeling of the degradation is not suitable for the mixture of PET/PA6. The data of the TG experiments only covering mass loss of the sample limit further analyses of the interaction and its mechanism.

Blends of PET/LDPE, PET/PS, and PA6/LDPE are exemplarily shown for blends of Group I and Group II in Fig. 6. Hardly any interactions occur in blends of PA6 and

Group I polymers. The RMSD between the experimental and modeled results of those polymers indicates high accuracy. The superposition approach is therefore considered to be valid. The selective degradation mechanism and degradation products of PA6 appear to only interact marginally with the radical mechanism of Group I polymers. For the volatile formation rate of PA6/LDPE blends in Fig. 6B, only one peak is detectable. This is attributed to the similar onset temperatures of both polymers. In blends with other Group I polymers, like HDPE or ABS two distinct overlapping peaks are noticeable. This reflects similar degradation behavior with a degradation onset dependency as identified for Group I blends.

With PET, which tends to form coke, different behavior is obtained. It degrades slightly faster in the presence of ABS
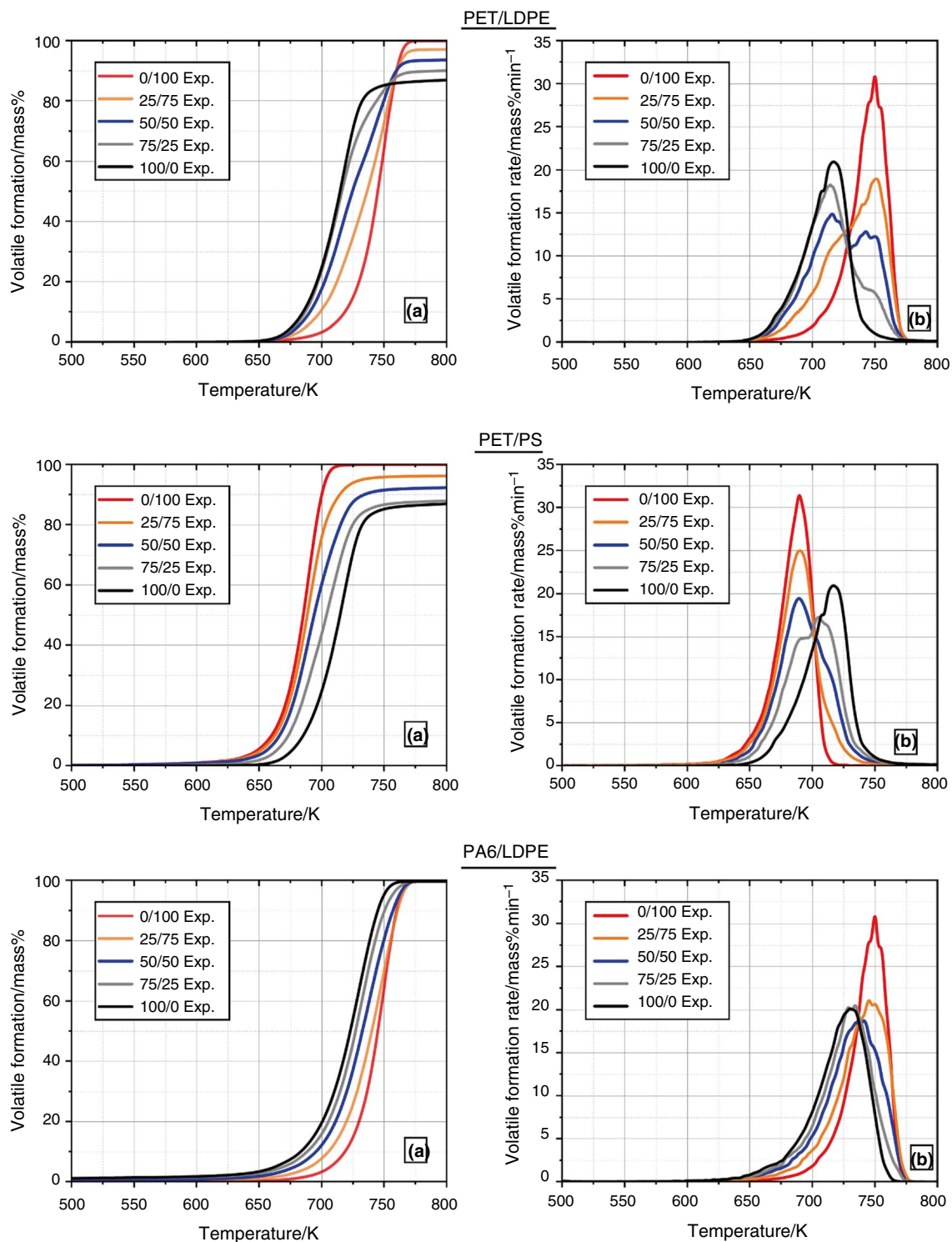
Fig. 6 Volatile formation **A** and its formation rate **B** from particular PET/LDPE, PET/PS, and PA6/LDPE blends in the ratio of 0/100, 25/75, 50/50, 75/25, and 100/0 mass% at a heating rate of 10 K min^{-1}

or PS. Both polymers have a lower onset of degradation. The solid residue mass is disproportionately increased in the blends as shown in Table 4. The coke formation tendency may be caused by coke precursors. These precursors usually consist of unsaturated, cyclic compounds [54]. Styrene is the main product of PS and ABS [18, 55]. Presumably, the structure of styrene allows it to enhance interaction with the coke precursors formed in PET degradation. This may

lead to increased solid residue in blends of PET with PS and ABS. However, blends of PET with polyolefins differ from this observation. The somewhat earlier degradation of PET slightly accelerates the pyrolysis of LDPE, HDPE, and PP. The greater the onset temperature difference, the more pronounced becomes the effect. In contrast to PET blends with styrene-containing polymers, the residue mass corresponds approximately to the linear postponed value. The acceleration can be observed, especially with low PET contents.

The results shown in Fig. 7 indicate only a slight reaction kinetic-specific interaction between Group I polymers and PVC. Both, the first and second degradation stages of PVC remain unchanged as exemplarily described for PVC/LDPE and PVC/PS blends in the volatile formation curve. The modeled results represent the degradation of the first two stages accurately. Even though degradation curve modeling in this range appears correctly, the interaction effects emerge in the third degradation stage from 690 to 775 K. In this range, the degradation is delayed for both blends. Similar results were observed for other Group I polymers. The effect leads to slightly higher RMSD values for these binary mixtures, e.g., up to 3.8 mass% for LDPE/PVC or 3.7 mass% for PS/PVC.

Table 4 Comparison of solid residue mass of PET blends at 873 K determined experimentally with particle samples and calculated via superposition

Polymer blend/mass%		Experimental solid residue[a] mass%	Solid residue[1] by superposition/ mass%
PET/LDPE	0/100	0.0 ± 0.07	0.0
	25/75	2.6[b]	3.0
	50/50	5.9 ± 0.28	6.0
	75/25	9.2[b]	9.0
	100/0	12.0 ± 0.29	12.0
PET/PS	0/100	0.0 ± 0.05	0.0
	25/75	3.5[b]	3.0
	50/50	7.1 ± 0.31	6.0
	75/25	11.3[b]	9.0
	100/0	12.0 ± 0.29	12.0
PET/ABS	0/100	0.3 ± 0.08	0.3
	25/75	3.8[b]	3.2
	50/50	7.0 ± 0.05	6.2
	75/25	11.0 ± 0.10	9.1
	100/0	12.0 ± 0.29	12.0
PET/PVC	0/100	6.6 ± 0.38	6.6
	25/75	9.1[b]	8.0
	50/50	10.0 ± 0.33	9.3
	75/25	11.2 ± 0.08	10.7
	100/0	12.0 ± 0.29	12.0

[a]Determined at 873 K with particular samples

[b]Standard deviation not calculable

In addition to Fig. 7, the experimentally determined solid residue is compared to the amount of solid residue calculated via superposition in Table 5. For PVC/LDPE blends, the value matches. A significant increase of solid residue mass is evident for particle PVC/PS blends. Li et al. reported the degradation of the polyene chains to mono- or polyaromatic hydrocarbons and additionally coke in the third degradation stage of PVC. This coke is formed by restructuring the unsaturated polyene intermediates [54]. Styrene, with its aromatic ring and the allyl group bound to it, features a similar structure. Therefore, Dodson and McNeill conclude that the interaction of the PS degradation products with the PVC coke precursors leads to the delay in the third degradation step [56]. The reactive styrene is more likely to react with the polyenes to form coke in this stage than the long-chain paraffinic products of the polyolefins LDPE, HDPE, and PP. Nevertheless, also polyolefins share the effect of a minor reaction delay. The solid residue determined in ABS experiments supports this explanation. In ABS pyrolysis, styrene is also formed as main degradation product. ABS as a copolymer also contains acrylonitrile and butadiene structures. Therefore, a similar effect occurs as with PS, but to a reduced extent.

No dependence of the interactions on the potential polymer interface is identified by comparing particular and powder samples. It must be considered that PVC is only available as a powder for the experiments. The particular samples with PVC exhibit a more homogeneous blend as investigated for other blends. Therefore, differences are expected to be less prominent comparing these samples. Additionally, material homogenization processes such as diffusion may already occur before the effect becomes apparent at the end of the degradation reaction. Such processes could eliminate the influence of sample homogenization.

Distinct interactions become apparent in blends of PVC and the heteroatom-containing Group II polymers PET and PA6. The significant changes lead to high RMSD values, e.g., for PET/PVC of maximal 5.9 mass% and PA6/PVC of maximal 13.5 mass%. Consequently, the superposition approach is not valid for these binary mixtures. The characteristic three-stage mechanism of PVC is no longer visible. In contrast, the second degradation stage of PVC is more pronounced which is indicated by increasing volatile formation rates between 590 and 650 K in Fig. 8B. More sample reacts in this temperature range which shifts the typical plateau of PVC before the last degradation stage at about 690 K shown in Fig. 8A. This effect is underlined by the increased peak in the volatile formation rate at about 600 K. The rise from about 3 mass% min^{-1} to a maximum of 7 mass% min^{-1} is visible for all PVC/PET samples independently from the polymer proportions. In the volatile formation rate, elevated volatile formation rates in the temperature range of 600–675 K are present.
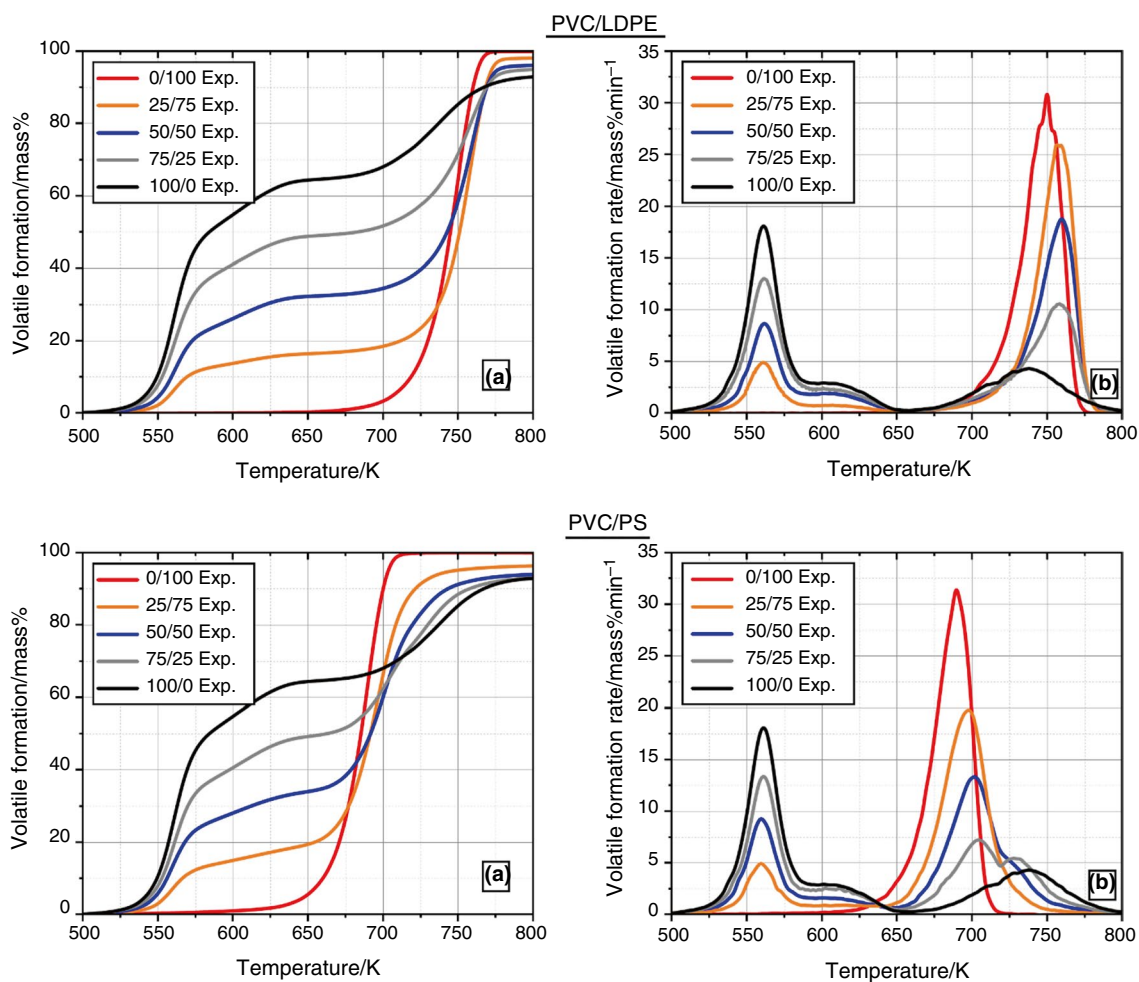
Fig. 7 Volatile formation **A** and its formation rate **B** from particular PVC/LDPE and PVC/PS blends in the ratio of 0/100, 25/75, 50/50, 75/25, and 100/0 mass% at a heating rate of 10 K min^{-1}

This confirms the conclusion of Chia et al. [57]. They report that HCl molecules formed in the primary degradation stage of PVC accelerate the degradation of PET. Considering the ionic degradation mechanism of PET and PA6, an interaction with HCl appears plausible. Yet, the start and end of the degradation of the mixtures remain predictable by model calculations. Solid residue formation increases disproportionately in the mixtures, similar to PS and PET blends. Intermediate products from polyene degradation and PET precursors may react to form new molecules, which form solid products as residues.

The volatile formation in Fig. 9 demonstrates deviating experimental results compared to modeled data and control experiments. While the RMSD of control experiments with model results is in the margin of error (<2 mass%), the samples in a shared reaction room feature significant interactions. Strong acceleration of the reaction is evident. The volatile formation in the particle and powder samples of PVC/PET before 650 K accounts for approx. 50 mass%, while it is

only 35 mass% in the model or the experiments with divided crucibles. Similar results are obtained with PA6/PVC blends. Approx. 60 mass% of volatiles are formed in the particle or powder samples. The experimental results with divided crucibles or the model results only show 35% of volatile below 650 K. The acceleration in blends of Group II and PVC is slightly increased for the powders in comparison with the particle sample. Again, it has to be considered that PVC is provided as powder. Therefore, particular samples are assumed to vary less as the reaction interface is supposedly similar. In the case of PVC/PET, increased fluctuations in the individual measurements of powder and particle samples are observed. Therefore, a significant influence of the molecular proximity can neither be confirmed nor disproved for PVC/PET and PVC/PA6 blends in a ratio of 50/50 mass% at heating rates of 10 K min^{-1} within this study.

Table 5 Comparison of solid residue mass of PVC blends at 873 K determined experimentally with particle samples and calculated via superposition

Polymer blend/mass%		Experimental solid residue[a] mass%	Solid residue[a] by superposition/ mass%
PVC/LDPE	0/100	0.0 ± 0.05	0.0
	25/75	1.8[b]	1.7
	50/50	3.7 ± 0.15	3.3
	75/25	4.8 ± 0.10	5.0
	100/0	6.6 ± 0.38	6.6
PVC/PS	0/100	0.0 ± 0.04	0.0
	25/75	3.4[b]	1.7
	50/50	5.7 ± 0.08	3.3
	75/25	6.6[b]	5.0
	100/0	6.6 ± 0.38	6.6
PVC/ABS	0/100	0.3 ± 0.08	0.3
	25/75	2.7 ± 0.10	1.9
	50/50	4.4 ± 0.07	3.5
	75/25	6.1[b]	5.0
	100/0	6.6 ± 0.38	6.6

[a]Determined at 873 K with particular samples

[b]Standard deviation not calculable

Complex polymer blends

The TG data of Mix 1 and Mix 2 allow validation of the effects found in the binary blend study in a more complex feedstock composition. As stated in Sect. "Materials and experimental Methods", Mix 1 consists only of polymers from Group I. Those polymers show no significant interactions in binary mixtures. Therefore, their degradation in blends is assumed to be correctly modeled with the superposition approach. In contrast, Mix 2 contains all polymers investigated in this work. Significant deviations between the model and experiment are to be expected, considering the previously identified interactions of Group II polymers and PVC. A comparison of the modeled and the experimental volatile formation is shown in Fig. 10.

Both the experimental and modeled degradations of Mix 1 reveal similar results. The RMSD for the experiment of Mix 1 accounts for 1.3 mass%, indicating high modeling accuracy. The degradation starts at approximately 620 K

and ends at approximately 770 K. Minor differences in the degradation curves account for the uncertainties of different experiments and the model data. These results indicate that the model calculates reliable degradation kinetics in dynamic TG experiments for polymers in Group I. The effect of slightly accelerated polyolefin degradation induced by radicals of the PS or ABS degradation is visible. Nevertheless, neglectable polymer interaction in the degradation mechanism is identified for LDPE, HDPE, PP, PS, and ABS regarding the reaction kinetics. This validates the conclusions from the systematic study of binary mixtures.

The degradation modeling of Mix 2 needs to be evaluated at different curve sections. Comparable behavior is obtained at the beginning and the end of the degradation by experimental data and model calculations. The final degradation of the linear carbon backbone of polyolefin chains and the polyene intermediates of PVC is well described via superposition. The formation of solid residue in the experiment and the model is similar. The experiment reveals a somewhat higher solid residue in contrast to the model data. This effect was already observed with blends of PVC and PET with other polymers like PS. Between 590 and 670 K, a new peak in the volatile formation rate is present, leading to a significant acceleration of the volatile formation in the experiments. The third degradation section ranges from 670 to 725 K. This range possibly represents the degradation of PET, PA6, PS, and ABS. The RMSD for Mix 2 of 4.6 exceeds the margin of error and therefore indicates the significant interactions. Consequently, the model fails to represent the degradation correctly as a result of the interactions, for example, of the PVC intermediates with, PET or PA6. As expected, the superposition approach is inadequate for simulating the entire reaction process of such heteroatom-containing polymer blends. Nevertheless, the model correctly calculates the start and end of the degradation even for such a complex mixture with obvious interactions of polymers. Regarding the solid residue from the experiment, comparable but slightly lower coke formation is calculated. In general, the results of Mix 1 and Mix 2 confirm the transferability of the effects concluded from binary mixtures. A study on superposition-based modeling of pyrolysis energy demand shows comparable dependencies on the superposition approach toward comparable polymer mixtures [58].
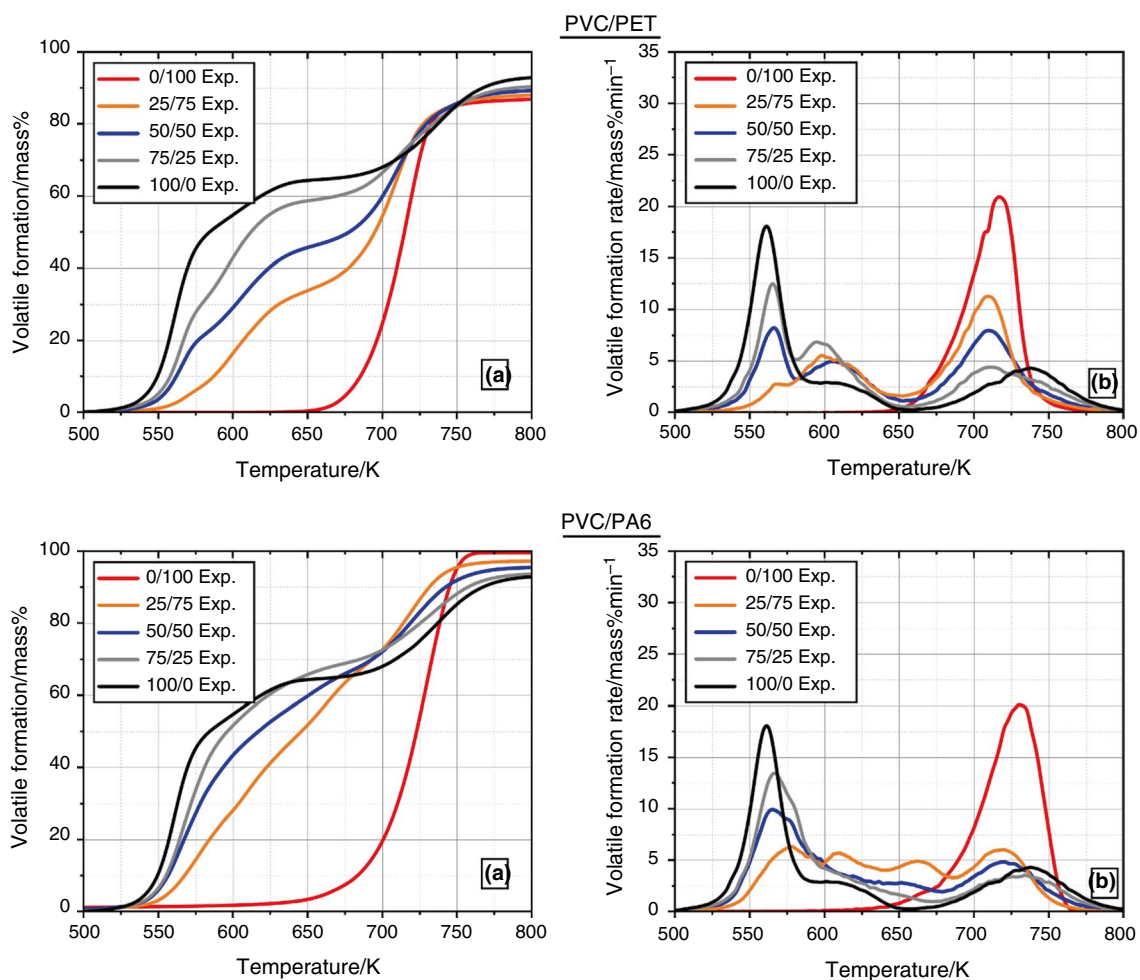
Fig. 8 Volatile formation **A** and its formation rate **B** from particular PVC/PET and PVC/PA6 blends in the ratio of 0/100, 25/75, 50/50, 75/25, and 100/0 mass% at a heating rate of 10 K min^{-1}
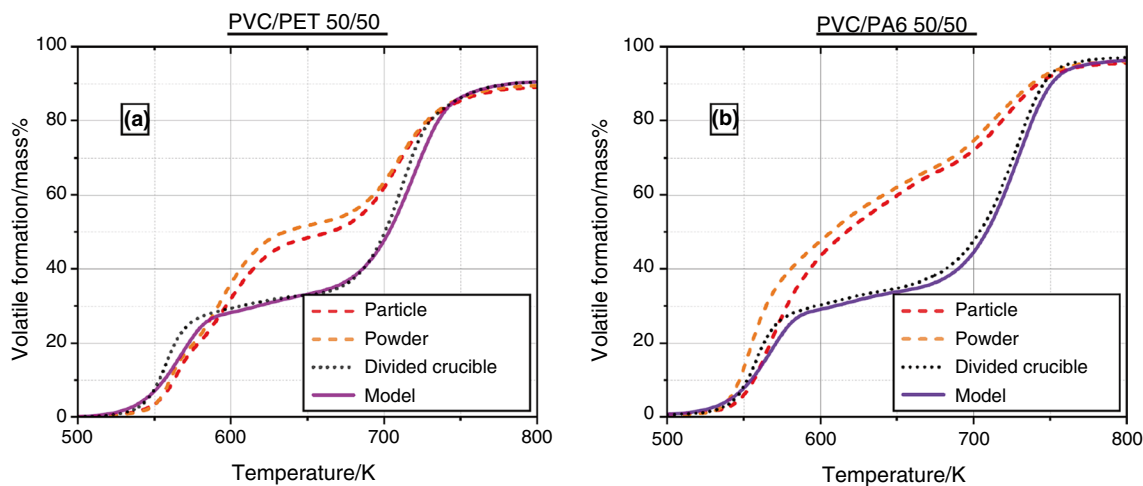
Fig. 9 Volatile formation of differently prepared PVC/PET **A** and PVC/PA6 **B** blend samples compared to modeled data in the ratio of 50/50 mass% at a heating rate of 10 K min^{-1}
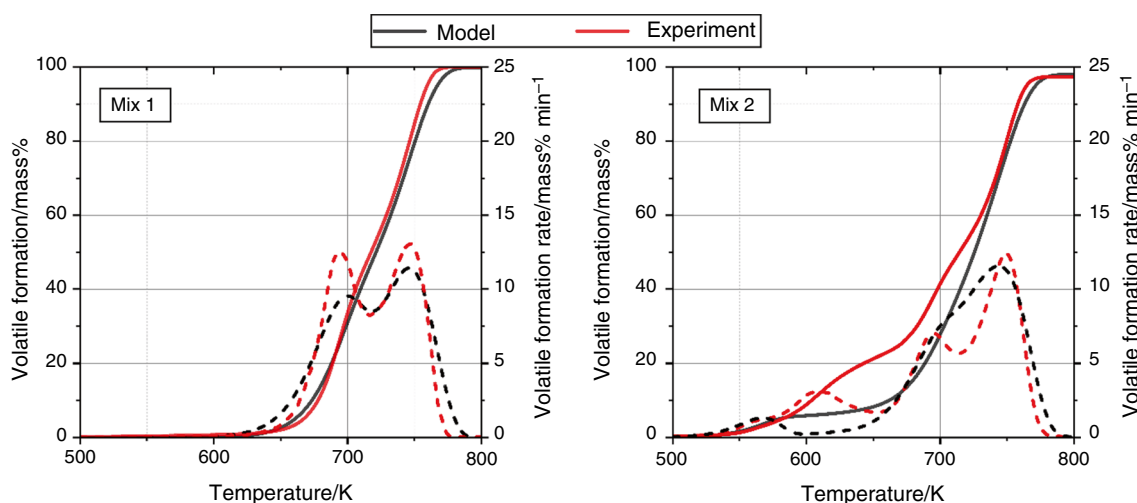
Fig. 10 Experimental and modeled volatile formation (continuous line) and volatile formation rate (dashed line) from the particular samples of Mix 1 and Mix 2 at a heating rate of 10 K min^{-1}

Conclusions

This systematic thermogravimetric study reveals different interaction effects and their significant dependency on the feedstock composition in the pyrolysis of mixed thermoplastics. From this, a grouping of thermoplastics depending on their chain structure is suggested. This chain structure, especially the type and location of heteroatoms, significantly influences the degradation mechanism. The interactions occur in the shared melt phase while degrading. Similar degradation mechanisms lead to comparable interaction effects of polymers in blends. The first group consisting of LDPE, HDPE, PP, PS, and ABS is characterized by a stable carbon–carbon chain backbone. In contrast, polymers in the second group contain heteroatoms in their main chain structure. Examples are the oxygenated ester bonds of PET and the nitrogen-containing peptide bonds of PA6. PVC represents an independent third group. Although PVC shares the carbon–carbon backbone of the first group polymers, the chlorine atoms exhibit electronegativity gradients of the bound side groups, leading to a differing degradation behavior. The observed polymer degradation interactions are group-dependent and lead to different effects of varying intensity. Increased coke formation and accelerated or delayed degradation reactions are observed in specific mixtures. Generally, the interactions are more pronounced with higher mixing homogeneity of the samples because of the increased potential interaction interface.

The evaluation of the model accuracy shows good accordance even though more complex polymer-specific models are expected to perform more precisely. The models' advantage mainly consists of the flexible adaptation to a multitude of thermoplastics while maintaining prediction quality. The

formation from thermoplastic blends of polymers featuring a carbon–carbon backbone is predicted well with the presented model. If heteroatom-containing polymers are present the occurring interactions change the degradation mechanisms.

Outlook

The study reveals further research demand for the characterization of interactions during the degradation of thermoplastic compounds. The precise identification of interaction reactions and reaction pathways requires comparative in-depth analyses of the resulting degradation products. For this purpose, experimental systems beyond thermogravimetry must be employed to overcome the methodological limitations of TG. Also, degradation intermediates and coke products should be analyzed in depth to characterize the interaction effects. Additional experimental methods (e.g., isothermal experiments) may contribute to evaluating the interaction dependencies in detail.

Various options for refining the superposition-based kinetic model are identified. In the case of interactions, a model adjustment in the form of an interaction term comparable to Hujuri et al. might be possible [36]. This model adjustment should allow for the simple implementation of further interaction effects. In addition, broadening the database by investigating further mixed plastic components, such as other polymer types, additives, or other waste components like biomass, would improve the prediction of complex plastic waste pyrolysis.

Supplementary Information

Two files provide more information on the comparison of the method of IPRM by Zeller et al. and the kinetic modeling of the virgin polymers by Kissinger–Akahira–Sunose method. File 1 shows activation energy and preexponential factor in dependence of the conversion rate of the pyrolysis reaction. File two provides the primary TG data which is the basis for the kinetic modeling. This SI file also shows eight additional figures that display the modeled and the primary experimental mass loss curves of each pure polymer (LDPE, HDPE, PP, PS, ABS, PET, PA6, and PVC) for different heating rates. Another file provides the data for the comparison of model results with experiments at 100 K min^{-1}. The fourth SI includes the RMSD values calculated for the entire experimental dataset and the corresponding model results generated in this study.

References

1. Keijer T, Bakker V, Slootweg JV. Circular chemistry to enable a circular economy. Nat Chem. 2019. https://doi.org/10.1038/s41557-019-0226-9.

2. European Parliament and the Council. Establishing the framework for achieving climate neutrality and amending regulations (EC) No 401/2009 and (EU) 2018/1999 ("European Climate Law"), 2021. https://eur-lex.europa.eu/eli/reg/2021/1119/oj. Accessed 9 Aug 2024

3. Rahimi A, García JM. Chemical recycling of waste plastics for new materials production. Nat Rev Chem. 2017. https://doi.org/10.1038/s41570-017-0046.

4. Van Geem KM. Plastic waste recycling is gaining momentum. Science. 2023. https://doi.org/10.1126/science.adj2807.

5. Arena U, Ardolino F. Technical and environmental performances of alternative treatments for challenging plastics waste. Resour Conserv Recycl. 2022. https://doi.org/10.1016/j.resconrec.2022.106379.

6. Arena U, Parrillo F, Ardolino F. An LCA answer to the mixed plastics waste dilemma: energy recovery or chemical recycling? Waste Manage. 2023. https://doi.org/10.1016/j.wasman.2023.10.011.

7. Volk R, Stallkamp C, Steins JJ, Yogish SP, Müller RC, Stapf D, Schultmann D. Techno-economic assessment and comparison of different plastic recycling pathways: a German case study. J Ind Ecol. 2021. https://doi.org/10.1111/jiec.13145.

8. Keller F, Voss RL, Lee RP, Meyer B. Life cycle assessment of global warming potential of feedstock recycling technologies: case study of waste gasification and pyrolysis in an integrated inventory model for waste treatment and chemical production in Germany. Resour Conserv Recycl. 2022. https://doi.org/10.1016/j.resconrec.2021.106106.

9. Geyer R, Jambeck JR, Law KL. Production, use, and fate of all plastics ever made. Sci Adv. 2017. https://doi.org/10.1126/sciadv.1700782.

10. Lase IS, Tonini D, Caro D, Albizzati PF, Cristóbal J, Roosen M, Kusenberg M, Ragaert K, Van Geem KM, Dewulf J, De Meester S. How much can chemical recycling contribute to plastic waste recycling in Europe? An assessment using material flow analysis modeling. Resour Conserv Recycl. 2023. https://doi.org/10.1016/j.resconrec.2023.106916.

11. Ragaert K, Delva L, Van Geem KM. Mechanical and chemical recycling of solid plastic waste. Waste Manage. 2017. https://doi.org/10.1016/j.wasman.2017.07.044.

12. Lase IS, Bashirgonbadi A, Van Rhijn F, Dewulf J, Ragaert K, Delva L, Roosen M, Brandsma M, Langen M, De Meester S. Material flow analysis and recycling performance of an improved mechanical recycling process for post-consumer flexible plastics. Waste Manage. 2022. https://doi.org/10.1016/j.wasman.2022.09.002.

13. Brouwer MT, Van Thoden Velzen EU, Ragaert K, Ten Klooster R. Technical limits in circularity for plastic packages. Sustainability. 2020. https://doi.org/10.3390/su122310021.

14. PlasticsEurope, Plastics—The facts 2021. An analysis of European plastics production, demand and waste data, Brussels, 2022. https://plasticseurope.org/knowledge-hub/plastics-the-facts-2022/. Accessed 9 Aug 2024

15. Bockhorn H, Hornung A, Hornung U, Schawaller U. Kinetic study on the thermal degradation of polypropylene and polyethylene. J Anal Appl Pyrolysis. 1999. https://doi.org/10.1016/S0165-2370(98)00131-4.

16. Faravelli T, Pinciroli M, Pisano F, Bozzano G, Dente M, Ranzi E. Thermal degradation of polystyrene. J Anal Appl Pyrolysis. 2001. https://doi.org/10.1016/S0165-2370(00)00159-5.

17. Wall LA, Straus S. Pyrolysis of polyolefins. J Polym Sci. 1960. https://doi.org/10.1002/pol.1960.1204414404.

18. Suzuki M, Wilkie CA. The thermal degradation of acrylonitrile-butadiene-styrene terpolymer as studied by TGA/FTIR. Polym Degrad Stab. 1995. https://doi.org/10.1016/0141-3910(94)00122-O.

19. Jenekhe SA, Lin JW, Sun B. Kinetics of the thermal degradation of polyethylene terephthalate. Thermochim Acta. 1983. https://doi.org/10.1016/0040-6031(83)80283-4.

20. Montaudo G, Puglisi C, Samperi F. Primary thermal degradation mechanisms of PET and PBT. Polym Degrad Stab. 1993. https://doi.org/10.1016/0141-3910(93)90021-A.

21. Straus S, Wall LA. Pyrolysis of polyamides. J Res Natl Inst Stand. 1958;60:39–45.

22. Bockhorn H, Hornung A, Hornung U, Weichmann J. Kinetic study on the non-catalysed and catalysed degradation of polyamide 6 with isothermal and dynamic methods. Thermochim Acta. 1999. https://doi.org/10.1016/S0040-6031(99)00151-3.

23. Yu J, Sun L, Ma C, Qiao Y, Yao H. Thermal degradation of PVC: a review. Waste Manage. 2016. https://doi.org/10.1016/j.wasman.2015.11.041.

24. Marongiu A, Faravelli T, Bozzano G, Dente M, Ranzi E. Thermal degradation of poly(vinyl chloride). J Anal Appl Pyrolysis. 2003. https://doi.org/10.1016/S0165-2370(03)00024-X.

25. Zeller M, Garbev K, Weigel L, Saatzer T, Merz D, Tavakkol S, Stapf D. Thermogravimetric studies, kinetic modeling and product analysis of the pyrolysis of model polymers for technical polyurethane applications. J Anal Appl Pyrolysis. 2023. https://doi.org/10.1016/j.jaap.2023.105976.

26. Aboulkas A, El Harfi K, El Bouadili A. Thermal degradation behaviors of polyethylene and polypropylene. Energy Conv Manage. 2010. https://doi.org/10.1016/j.enconman.2009.12.017.

27. Westerhout RWJ, Kuipers JAM, Van Swaaij WPN. Experimental determination of the yield of pyrolysis products of polyethene and polypropene: influence of reaction conditions. Ind Eng Chem Res. 1998. https://doi.org/10.1021/ie970384a.

28. Costa P, Pinto F, Ramos AM, Gulyurtlu I, Cabrita I, Bernardo MS. Study of the pyrolysis kinetics of a mixture of polyethylene, polypropylene, and polystyrene. Energy Fuels. 2010. https://doi.org/10.1021/ef101010n.

29. Faravelli T, Bozzano G, Colombo M, Ranzi E, Dente D. Kinetic modeling of the thermal degradation of polyethylene and polystyrene mixtures. J Anal Appl Pyrolysis. 2003. https://doi.org/10.1016/S0165-2370(03)00058-5.

30. Wu J, Chen T, Luo X, Han D, Wang Z, Wu J. TG/FTIR analysis on co-pyrolysis behavior of PE. PVC and PS Waste Manage. 2014. https://doi.org/10.1016/j.wasman.2013.12.005.

31. Genuino HC, Pilar Ruiz M, Heeres HJ, Kersten SRA. Pyrolysis of mixed plastic waste: predicting the product yields. Waste Manage. 2023. https://doi.org/10.1016/j.wasman.2022.11.040.

32. La Mantia FP, Morreale M, Botta L, Mistretta MC, Ceraulo M, Scaffaro R. Degradation of polymer blends: a brief review. Polym Degrad Stab. 2017. https://doi.org/10.1016/j.polymdegradstab.2017.07.011.

33. Pek WK, Ghosh UK. Effect of binary mixture of waste plastics on the thermal behavior of pyrolysis process. Environ Prog Sustain Energy. 2015. https://doi.org/10.1002/ep.12087.

34. Chowlu ACK, Reddy PK, Ghoshal AK. Pyrolytic decomposition and model-free kinetics analysis of mixture of polypropylene (PP) and low-density polyethylene (LDPE). Thermochim Acta. 2009. https://doi.org/10.1016/j.tca.2008.12.004.

35. Klaimy S, Lamonier JF, Casetta M, Heymans S, Duquesne S. Recycling of plastic waste using flash pyrolysis—Effect of mixture composition. Polym Degrad Stab. 2021. https://doi.org/10.1016/j.polymdegradstab.2021.109540.

36. Hujuri U, Ghoshal AK, Gumma S. Modeling pyrolysis kinetics of plastic mixtures. Polym Degrad Stab. 2008. https://doi.org/10.1016/j.polymdegradstab.2008.07.006.

37. Miranda R, Pakdel H, Roy C, Vasile C. Vacuum pyrolysis of commingled plastics containing PVC II product analysis. Polym Degrad Stab. 2001. https://doi.org/10.1016/S0141-3910(01)00066-0.

38. Tuffi R, D'Abramo S, Cafiero LM, Trinca E, Vecchio CS. Thermal behavior and pyrolytic degradation kinetics of polymeric mixtures from waste packaging plastics. Express Polym Lett. 2018. https://doi.org/10.3144/expresspolymlett.2018.7.

39. Vyazovkin S, Burnham AK, Criado JM, Pérez-Maqueda LA, Popescu C, Sbirrazzuoli N. ICTAC Kinetics Committee recommendations for performing kinetic computations on thermal analysis data. Thermochim Acta. 2011. https://doi.org/10.1016/j.tca.2011.03.034.

40. Capone C, Di Landro L, Inzoli F, Penco M, Sartore L. Thermal and mechanical degradation during polymer extrusion processing. Polym Eng Sci. 2007. https://doi.org/10.1002/pen.20882.

41. Schweighuber A, Felgel-Farnholz A, Bögl T, Fischer J, Buchberger W. Investigations on the influence of multiple extrusion on the degradation of polyolefins. Polym Degrad Stab. 2021. https://doi.org/10.1016/j.polymdegradstab.2021.109689.

42. Jomaa G, Goblet P, Coquelet C, Morlot V. Kinetic modeling of polyurethane pyrolysis using non-isothermal thermogravimetric analysis. Thermochim Acta. 2015. https://doi.org/10.1016/j.tca.2015.05.009.

43. Gotor FJ, Criado JM, Malek J, Koga N. Kinetic analysis of solid-state reactions: the universality of master plots for analyzing isothermal and nonisothermal experiments. J Phys Chem. 2000;104:10777–82. https://doi.org/10.1021/jp0022205.

44. Criado JM. Kinetic analysis of DTG data from master curves. Thermochim Acta. 1978. https://doi.org/10.1016/0040-6031(78)85151-X.

45. The MathWorks Inc. Global optimization toolbox user's guide. 2023. https://de.mathworks.com/help/gads/direct-search.html. Accessed 9 Aug 2024

46. Al-Salem SM, Antelava A, Constantinou A, Manos G, Dutta A. A review on thermal and catalytic pyrolysis of plastic solid waste (PSW). J Environ Manage. 2017. https://doi.org/10.1016/j.jenvman.2017.03.084.

47. Encinar JM, González JF. Pyrolysis of synthetic polymers and plastic wastes: kinetic study. Fuel Process Tech. 2008. https://doi.org/10.1016/j.fuproc.2007.12.011.

48. Knümann R, Bockhorn H. Investigation of the kinetics of pyrolysis of PVC by TG-MS-Analysis. Combust Sci Tech. 1994. https://doi.org/10.1080/00102209408951877.

49. Marcilla A, Beltrán M. Thermogravimetric kinetic study of poly(vinyl chloride) pyrolysis. Polym Degrad Stab. 1995. https://doi.org/10.1016/0141-3910(95)00050-V.

50. Yang J, Miranda R, Roy C. Using the DTG curve fitting method to determine the apparent kinetic parameters of thermal decomposition of polymers. Polym Degrad Stab. 2001. https://doi.org/10.1016/S0141-3910(01)00129-X.

51. Wu CH, Chang CY, Hor JL, Shih SM, Chen LW, Chang FW. On the thermal treatment of plastic mixtures of MSW: pyrolysis kinetics. Waste Manage. 1993. https://doi.org/10.1016/0956-053X(93)90046-Y.

52. Nait-Ali LK, Colin X, Bergeret A. Kinetic analysis and modelling of PET macromolecular changes during its mechanical recycling by extrusion. Polym Degrad Stab. 2011. https://doi.org/10.1016/j.polymdegradstab.2010.11.004.

53. Lüderwald I, Aguilera C. Catalytic degradation of polymers, 2. Nylon 6. Makromol Chem Rapid Commun. 1982. https://doi.org/10.1002/marc.1982.030030516.

54. Li D, Lei S, Wang P, Zhong L, Ma W, Chen G. Study on the pyrolysis behaviors of mixed waste plastics. Renew Energy. 2021;173:662–74. https://doi.org/10.1016/j.renene.2021.04.035.

55. Faravelli T, Bozzano G, Scassa G, Perego M, Fabini S, Ranzi E, Dente M. Gas product distribution from polyethylene pyrolysis. J Anal Appl Pyrolysis. 1999. https://doi.org/10.1016/S0165-2370(99)00032-7.

56. Dodson B, McNeill IC. Degradation of polymer mixtures: VI. Blends of poly (vinyl chloride) with polystyrene. J Polym Sci Polym Chem. 1976. https://doi.org/10.1002/pol.1976.170140208.

57. Chia JWF, Sawai O, Nunoura T. Reaction pathway of poly(ethylene) terephthalate carbonization: decomposition behavior based on carbonized product. Waste Manage. 2020. https://doi.org/10.1016/j.wasman.2020.04.035.

58. Netsch N, Zeller M, Richter F, Bergfeldt B, Tavakkol S, Stapf D. Energy demand for pyrolysis of mixed thermoplastics and waste plastics in chemical recycling: model prediction and pilot-scale validation. ACS Sustain Resour Manage. 2024. https://doi.org/10.1021/acssusresmgt.4c00109.

Authors and Affiliations

N. Netsch[1] · **L. Schröder**[1] · **M. Zeller**[1] · **I. Neugber**[1] · **D. Merz**[1] · **C. O. Klein**[2] · **S. Tavakkol**[1] · **D. Stapf**[1]

✉ N. Netsch
Niklas.Netsch@kit.edu

S. Tavakkol
Salar.Tavakkol@kit.edu

[1] Institute for Technical Chemistry (ITC), Karlsruhe Institute of Technology (KIT), Kaiserstraße 12, 76131 Karlsruhe, Germany

[2] Institute for Chemical Technology and Polymer Chemistry (ITCP), Karlsruhe Institute of Technology (KIT), Kaiserstraße 12, 76131 Karlsruhe, Germany